A Novel Conformal Surface Current Technique for Large Problems Based on High-Performance Parallel FDTD Method

Jian Wang, Wen-Yan Yin, *Senior Member, IEEE*, and Yin-Shui Xia

***Abstract*—Solution of electrically large problems such as scattering and diffraction by large objects—e.g., missiles, ships, and aircraft—is of considerable interest today. The finite-difference time-domain (FDTD) method is a versatile tool that has been extensively applied to the solution of these large problems. However, since the FDTD algorithm usually works with a Cartesian grid, it is not very well suited for extracting information on the induced current distribution on the surface of the object. Given this background, our objective in this letter is to describe a novel conformal technique, applied in conjunction with the high-performance parallel FDTD method, which extracts and displays the information of the surface on an arbitrarily shaped object in an accurate and efficient manner. Finally, some typical numerical examples are given to demonstrate the capability of our developed conformal technique.**

***Index Terms*—Conformal surface current, electrically large problems, parallel finite-difference time-domain (FDTD) method.**

I. Introduction

IN MANY electromagnetic applications such as electromagnetic compatibility (EMC), microwave device design, radar scattering, etc., the knowledge of the surface current is of considerable instant for characterizing the complex electromagnetic systems [1], [2]. This is because the knowledge of the surface current provides useful and valuable information for further predicting and protecting the electromagnetic interference (EMI) effects in various electronic systems.

In the rapid progress in computational electromagnetic (CEM) solvers, the finite-difference time-domain (FDTD) solver [3] remains a popular choice for solving complex and electromagnetic systems because of its versatility and ability to solve large ones by using parallelization techniques [4], [5]. However, unlike the method of moments (MoM) [6], [7], the FDTD algorithm is designed to work with electric and magnetic fields distributions, and hence it is not very well suited for extracting the information on the induced current distribution from the field solution. Moreover, some commercial software packages, such as FEKO [8] and CST [9], can give the surface current results of arbitrary objects. Unfortunately, most of them are not good at parallel efficiency or in solving the wideband problems. Our objective in this letter is to present a novel scheme for extracting as well as displaying the induced current distribution, accurately and efficiently, from the field solution generated by the FDTD algorithm. We also show how to combine the power of visualization tools to display the current distribution computed by using the technique mentioned above. Toward this end, we take advantage of the recent availability of a high-performance parallel algorithm with which we can implement our code to solve some real large problems on a ship platform. The detailed description of the parallel algorithm used here is shown in our former work [10], in which we just need to exchange only the $\boldsymbol{H}$-fields between the adjacent subdomains and the $\boldsymbol{E}$-fields on the interface should be updated in both subdomains.

The letter is organized as follows. Section II describes the procedure for evaluating the surface current. Next, some typical numerical examples are presented in Section III to demonstrate both the efficiency and the versatility of the proposed technique when applied to electrically large and complex objects. Finally, some conclusions and observations are included in Section IV.

II. Conformal Surface Current Calculation

In this section, we present a detailed description of the implementation of the proposed surface current extraction technique that is useful for analyzing the EMC/EMI phenomena in electrically large and complex objects.

A. Problem Description

Fig. 1 shows a perfect electric conductor (PEC) object illuminated by an EMI source, and our objective is to extract the surface current induced on the object when illuminated by the above source and analyzed by using the FDTD. The current at the point P located on the surface of the PEC object can be computed from the knowledge of the $\boldsymbol{H}$-field by using

$$\boldsymbol{J} = \boldsymbol{n} \times \boldsymbol{H} \tag{1}$$

where $\boldsymbol{n}$ and $\boldsymbol{H}$ are the normal to the surface and the magnetic field strength at P, respectively. We employ a high-performance parallel FDTD method at hand to compute the $\boldsymbol{H}$-fields for the problem. However, the conformal currents on the curved surface cannot be obtained directly by using the FDTD method because

Manuscript received October 14, 2012; revised November 30, 2012; accepted December 11, 2012. Date of publication December 20, 2012; date of current version March 12, 2013. This work was supported by the National Natural Science Fund of China under Grants 60831002 and 61131001 and the EMC Laboratory, Pennsylvania State University.

J. Wang and Y.-S. Xia are with the School of Information Science and Engineering, Ningbo University, Ningbo 315211, China (e-mail: wangjian1@nbu.edu.cn; xiayinshui@nbu.edu.cn).

W.-Y. Yin is with the Center for Optical and EM Research, State Key Lab of MOI, Department of Optical Engineering, Zhe Jiang University, Hangzhou 310058, China (e-mail: wyyin@zju.edu.cn).

Color versions of one or more of the figures in this letter are available online at http://ieeexplore.ieee.org.

Digital Object Identifier 10.1109/LAWP.2012.2235812

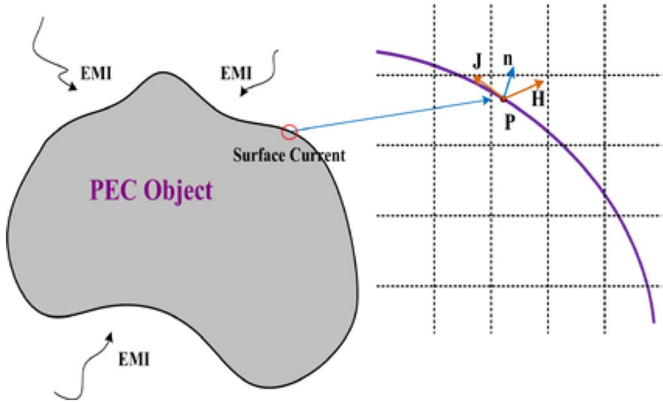

Fig. 1. Description for the generic surface current problems.

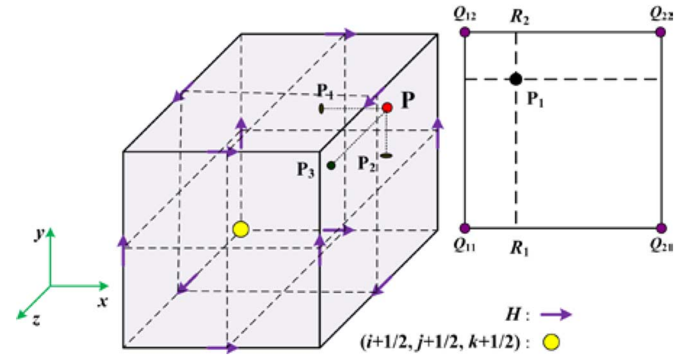

Fig. 2. Interpolation of the $\boldsymbol{H}$-field at P.

it works with a Cartesian grid, and it becomes necessary to interpolate this field between the computed values on points that do lie on the grid. In the real applications, we are also interested in looking at the surface distribution of the objects by utilizing a 3-D visualizing tool.

B. Implementation of the Methodology

There are two major steps involved in the extraction of the surface current distribution. The first step entails the modeling of the geometry of the object, which is followed by the computation of the magnetic field at the chosen point. We now proceed in detail as follows.

1) Description of the Model Surface: A common approach to modeling the surface is to use the triangular meshes to approximate the target surface. We can get the triangular mesh information, including the three-node coordinates and the index of each triangle mesh, from this description. In our method, we need to calculate the currents at all the vertices of index of each triangle mesh from this description. The current distribution can then be obtained by using interpolation schemes that utilize these discrete currents. The vertices normal vector can be calculated by using

$$\boldsymbol{n}_{\text{vertex}} = \sum_{i}^{N} \alpha_i \cdot \boldsymbol{n}_{\text{center}}^{i} \tag{2}$$

where $\boldsymbol{n}_{\text{center}}^{i}$ is the normal vector of the ith triangular around the considered vertex, and α_i is the ith angle related to the vertex point. $\boldsymbol{n}_{\text{center}}$ and α can be obtained by the three-node coordinates given by the triangular mesh information.

2) Computation of the $\boldsymbol{H}$-Field: The FDTD method yields the $\boldsymbol{H}$-field distribution at the Yee grids. First, we need to find the index that indicates the considered point that we can compute the H-field components required by the interpolation formula we intend to use. In our method, the H-field at P can be calculated by using the $\boldsymbol{H}$-field components in the x-, y-, and z-directions of the related cell. As shown in Fig. 2, P_1, P_2, and P_3 are the projection points of P in the three $\boldsymbol{H}$-field component planes. The $\boldsymbol{H}$-field component in x-direction at each point is given by

$$H_{R1} = \frac{d_{z1}}{\Delta z} H_x(Q_{11}) + \frac{d_{z2}}{\Delta z} H_x(Q_{12}) \tag{3a}$$

$$H_{R2} = \frac{d_{z1}}{\Delta z} H_x(Q_{21}) + \frac{d_{z2}}{\Delta z} H_x(Q_{22}) \tag{3b}$$

$$H_x(P_1) = \frac{d_{y1}}{\Delta y} H_{R1} + \frac{d_{y2}}{\Delta y} H_{R2} \tag{3c}$$

$$\begin{aligned} H_x(P_1) = {} & \frac{d_{y1}}{\Delta y} \left(\frac{d_{z1}}{\Delta z} H_x(Q_{11}) + \frac{d_{z2}}{\Delta z} H_x(Q_{12}) \right) \\ & + \frac{d_{y2}}{\Delta y} \left(\frac{d_{z1}}{\Delta z} H_x(Q_{21}) + \frac{d_{z2}}{\Delta z} H_x(Q_{22}) \right) \end{aligned} \tag{3d}$$

where d_y and d_z are the distance between P_1 and the H_x field points in y- and z-directions, respectively; Δy and Δz are the cell size in y- and z-directions, respectively.

The above interpolation formulas may need to be modified for some special cases. For instance, when some of the four $\boldsymbol{H}$-field components in one direction are equal to zero, under such circumstances, the $\boldsymbol{H}$-field components in the PEC region can be replaced by those in free space. Second, when we have all of the four $\boldsymbol{H}$-field components that are equal to zero, the interpolation formula becomes invalid and must be modified. One possible approach is to extend the interpolation domain and to use nine cells (16 field components in one direction). The interpolation formula can then be replaced by

$$H_x(P) = \sum_{u=1}^{N} \frac{1/d_u}{\sum\limits_{v=1}^{N} (1/d_v)} \cdot H_x(Q_u) \tag{4}$$

where N is the number of H_x points that are not equal to zero. d_c ($c = u$ and v) is the distance between the cth H_x field location and point P.

3) Computation of the Current: In our method, the point P is chosen to be located at the vertices of the surface triangular meshes. Furthermore, the current at P can be calculated by using the boundary condition formula based on the $\boldsymbol{H}$-field information, while the normal vector can be obtained from the previous steps. In frequency domain, the current can be expressed as

$$\begin{aligned} \boldsymbol{J}(\mathrm{P}, \omega_0) &= \boldsymbol{n}(P) \times \boldsymbol{H}(P, \omega_0) \\ &= \begin{pmatrix} \boldsymbol{e}_x & \boldsymbol{e}_y & \boldsymbol{e}_z \\ n_x(P) & n_y(P) & n_z(P) \\ H_x(P, \omega_0) & H_y(P, \omega_0) & H_z(P, \omega_0) \end{pmatrix} \end{aligned} \tag{5}$$

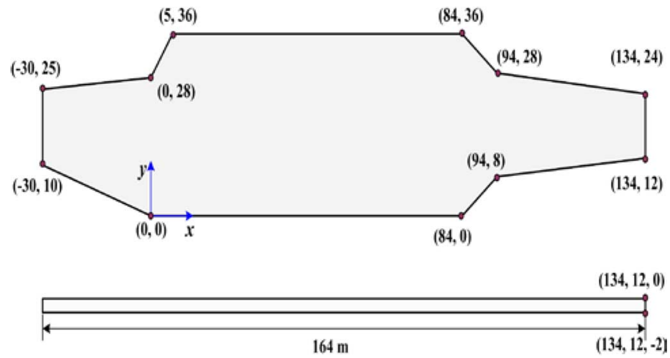

Fig. 3. Geometry of the ship deck.

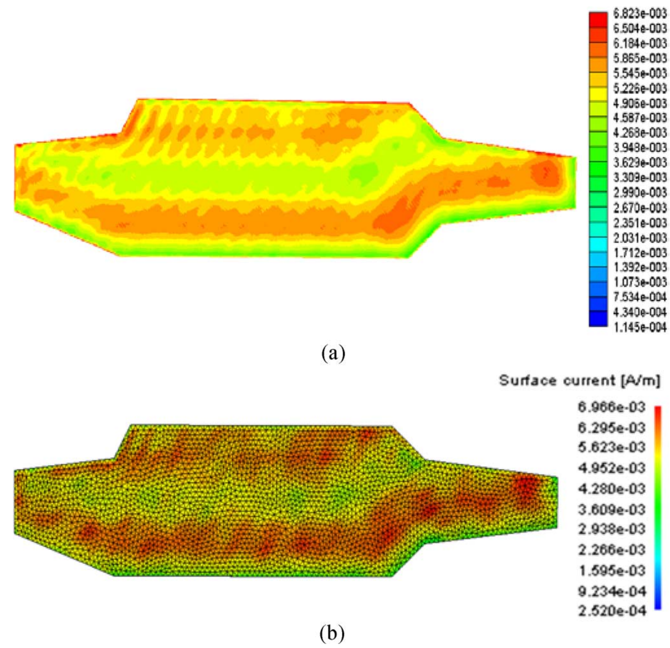

Fig. 4. Surface current on a ship deck: (a) proposed method and (b) FEKO result.

where e_u and $n_u(\boldsymbol{P})$ ($u = x, y$, and z) are the components of the unit vector and normal vector, respectively. The x-component of the current can be written as follows:

$$J_x(P, \omega_0) = n_y(P) \cdot H_z(P, \omega_0) - n_z(P) \cdot H_y(P, \omega_0). \quad (6)$$

We can now get the amplitude of $\boldsymbol{J}$ by using these current results though the current phase is not considered in our method. It could also be obtained if required.

4) Current Visualization: The first step toward the current visualization is to build a color map for integers between 0 and 255, where each integer is related to just one color. The currents can be mapped to integers between 0 and 255 based on the range of the current values at the vertices, and we can obtain the relationship between the current value and the color by looking up the color map. Furthermore, for the inner points of a triangle, the interpolation scheme based on barycentric coordinate is adopted to calculate the color value. As a result, a smooth and intuitive visualization effect can be achieved, which is helpful for investigating the EMC effects.

III. Numerical Results and Discussion

We have utilized the mathematical treatment described above, together with our high-performance parallel FDTD simulation tool, to carry out numerical computations that illustrate the accuracy and efficiency of our developed techniques. We now present them in the following.

A. Surface Current of a Large Ship Deck

The first example is a ship deck, shown in Fig. 3, which is illuminated by an electromagnetic pulse (EMP) signal. The object size is $164 \times 36 \times 2$ m^3. The incident wave propagates along the direction of $\varphi = 315°$ and $\theta = 45°$, with the polarization of $E_\theta = 1$ and $E_\varphi = 0$. We set the Fourier frequency of the current to be 150 MHz. The mesh size is $\Delta x = \Delta y = \Delta z = 10$ cm, and the computational domain is set to be $1660 \times 380 \times 40$. A six-layer perfectly matched layer (PML) boundary condition is used to truncate the six walls of the computational domain.

Fig. 4(a) and (b) compares the results for the current distributions calculated by our method and FEKO, respectively. In this example, the maximum difference between the results obtained by our method and those of FEKO is 0.143×10^{-3}. Therefore, the percentage error is less than 3% when the FEKO results are chosen as references. The comparison is good, and this is the further support for the accuracy testing of our method. Furthermore, the E_z component in time domain is captured by our method and CST at the observed point (134, 24, 2.5). The relative error of E_z obtained by these two methods is less than 2.3%. Table I shows the comparison of the memory, CPU time, and calculating error between the proposed method and CST. It is noted that our method has better parallel efficiency and less memory requirements compared to CST with similar accuracy.

TABLE I
Comparison of the Proposed Method and CST

Method	CPU time (Time steps=5000)		Memory	Calculating Error
	1 Core	4 Core		
Our Method	21 h 12min	5 h 48min	1.3 GB	2.3%
CST	19 h 8 min	7 h 34 min	3.2 GB	

We have run this test problem on a workstation with four CPUs (total 48 cores, each of them is AMD Opteron 6168 1.9 GHz). The simulation time on the four-CPU workstation using 48 cores is 1 h 33 min for 10 000 time-steps. The memory requirement for this problem is 1.3 GB. If we run the same problem by using only one core, the CPU time becomes 40 h 17 min. The parallel efficiency for 48 cores is 54.1%.

B. Surface Current of an Aircraft on a Carrier Platform

In the last example, we use the proposed approach to calculate the surface current distribution of an aircraft on a carrier. Fig. 5(a) and (b) shows the geometries of the problem. The ship size is $328 \times 72 \times 59$ m^3, as shown in Fig. 5(a). An aircraft as shown in Fig. 5(b), whose dimensions are $16 \times 8 \times 4$ m^3, is placed at a height of 2 m above the ship deck. We utilize a uniform mesh with $\Delta x = 15$ cm, $\Delta y = 12$ cm, and $\Delta z = 12$ cm, respectively. The target is illuminated by an external

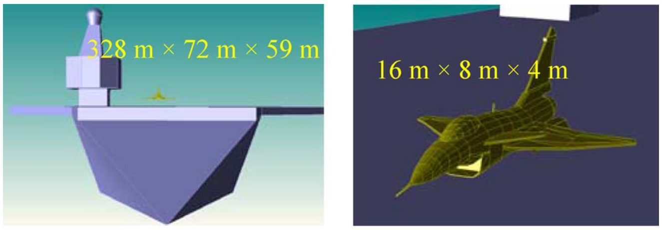

(a) (b)

Fig. 5. Geometry of the carrier platform. (a) Carrier platform. (b) Aircraft.

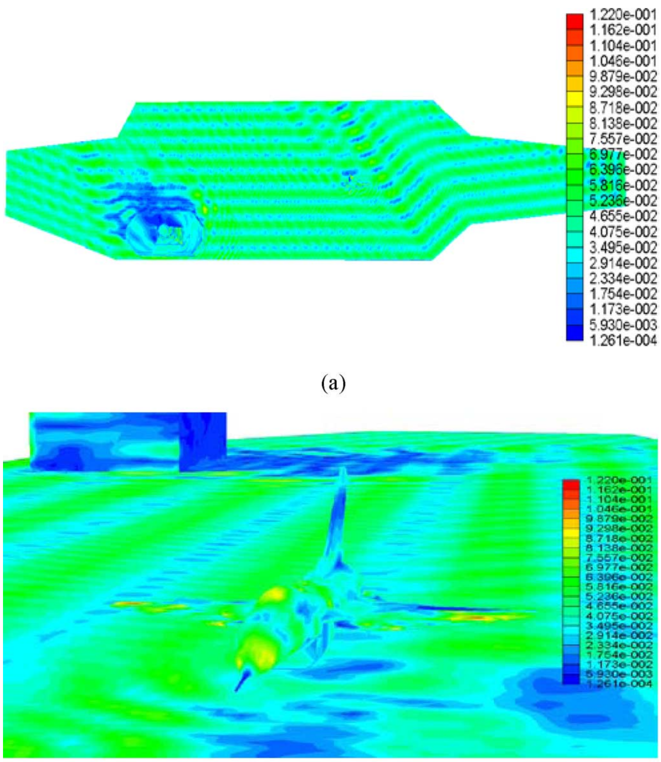

(a)

(b)

Fig. 6. Surface current on a war fleet: The incident wave propagates along the direction: $\varphi = 315^\circ$ and $\theta = 45^\circ$ with the polarization of $E_\theta = 1$ and $E_\varphi = 0$. (a) Carrier. (b) Aircraft.

EMP, which is along $\varphi = 315^\circ$ and $\theta = 45^\circ$ with the polarization of $E_\theta = 1$ and $E_\varphi = 0$. The obliquely incident EMP is described by a double-exponential function as follows:

$$E = E_0 k(e^{-\beta t} - e^{-\alpha t}) \tag{7}$$

with $k = 1.285$, $\alpha = 4.76 \times 10^8$, and $\beta = 3.0 \times 10^7$ chosen for our computation.

The simulation is carried out by using the FDTD code running on the platform a workstation with four CPUs (total 48 cores, each of them is AMD Opteron 6168 1.9 GHz), and it only requires 73 h to complete the simulation. The simulation process only requires less than 50 GB, and it only needs less than 3 GB memory to calculate the surface current by using a regular laptop. The surface current distributions at a frequency of 100 MHz are plotted in Fig. 6.

Fig. 6(a) shows the oblique incidence case in which there is an obvious shadow region behind the tower and the current distribution shows standing wave properties in the y-direction. There are also two shadow regions under the aircraft body and the right wing. We can see from Fig. 6(b) that the electromagnetic energy on the aircraft surface is concentrated on the two wings, the head, and the cabin.

IV. Conclusion

In this letter, we have presented a novel conformal surface current technique for handling electrically large problems illuminated by external EMPs that is based on the use of a high-performance parallel FDTD method. The proposed method uses the surrounding magnetic fields in at most 16 spatial discrete cells of the considered surface point to obtain the current by using an interpolation scheme as described above. Several real examples are given to demonstrate both accuracy and efficiency of our proposed novel conformal surface current technique for capturing current distribution of the complex and large objects. For example, in the last numerical test shown in Fig. 5, the FDTD computational domain is $2200 \times 600 \times 500$, and the memory requirement is approximate 50 GB. The proposed method only requires under 73 h for the simulation and under 10 min to calculate the surface current. We would like to conclude that our parallel FDTD code is both powerful and efficient in handling with very large EMC problems.

References

[1] M. Coenen, T. Maas, Y. Hu, and A. Roermund, "In-situ EMC testing using surface current sense wires," in *IEEE Int. Symp. Asia-Pacific Electromagn. Compat.*, Beijing, China, Apr. 2010, pp. 586–589.

[2] C. Borja and J. Romeu, "On the behavior of Koch island fractal boundary microstrip patch antenna," *IEEE Trans. Antennas Propagat.*, vol. 51, no. 6, pp. 1281–1291, June 2003.

[3] K. S. Yee, "Numerical solutions of initial boundary value problems involving Maxwell's equations in isotropic media," *IEEE Trans. Antennas Propagat.*, vol. AP-14, no. 5, pp. 302–307, May 1966.

[4] J. Z. Lei, C. H. Liang, W. Ding, and Y. Zhang, "Study on MPI-based parallel modified conformal FDTD for 3-D electrically large coated targets by using effective parameters," *IEEE Antennas and Wireless Propagat. Lett.*, vol. 7, pp. 175–178, 2008.

[5] C. Guiffaut and K. Mahdjoubi, "A parallel FDTD algorithm using the MPI library," *IEEE Antennas Propag. Mag.*, vol. 43, no. 2, pp. 94–103, Apr. 2001.

[6] J. Song, C. C. Lu, and W. C. Chew, "Multilevel fast multipole algorithm for electromagnetic scattering by large complex objects," *IEEE Trans. Antennas Propagat.*, vol. 45, no. 10, pp. 1488–1493, Oct. 1997.

[7] H. Bagcı, A. E. Yılmaz, J. M. Jin, and E. Michielssen, "Fast and rigorous analysis of EMC/EMI phenomena on electrically large and complex cable-loaded structures," *IEEE Trans. Electromagn. Compat.*, vol. 49, no. 2, pp. 361–381, May 2007.

[8] FEKO User's Manual Suite 5.5 EM Software & Systems-S. A. (Pty) Ltd., July 2009, [Online]. Available: [Online]. Available: http//www.feko.info

[9] CST Studio Suite 2010 CST Computer Simulation Technology, Nov. 2009, [Online] Available: [Online]. Available: http//www.cst.com

[10] W. Yu, X. Yang, Y. Liu, L. Ma, T. Su, N. Huang, R. Mittra, R. Maaskane, Y. Lu, Q. Che, R. Lu, and Z. Su, "A new direction in computational electromagnetics: Solving large problems using the parallel FDTD on the BlueGene/L supercomputer providing teraflop-level performance," *IEEE Antennas Propag. Mag.*, vol. 50, no. 2, pp. 26–44, Apr. 2008.